

APPLICATION OF THE U.S. HIGH CYCLE FATIGUE DATA BASE TO WIND TURBINE BLADE LIFETIME PREDICTIONS

Herbert J. Sutherland

Wind Energy Technology
Sandia National Laboratories
Albuquerque, NM 87185-0708
Phone: (505)844-2037
Fax: (505)845-9500
E-Mail: hjsuthe@sandia.gov

and

John F. Mandell

Department of Chemical Engineering
Montana State University
Bozeman, MT 59717
Phone: (406)994-4543
Fax: (406)994-5308

ABSTRACT

This paper demonstrates a methodology for predicting the service lifetime of wind turbine blades using the high-cycle fatigue data base for typical U.S. blade materials developed by Mandell, et al. (1995). The first step in the analysis is to normalize the data base (composed primarily of data obtained from specialized, relatively small coupons) with fatigue data from typical industrial laminates to obtain a Goodman Diagram that is suitable for analyzing wind turbine blades. The LIFE2 fatigue analysis code for wind turbines is then used for the fatigue analysis of a typical turbine blade with a known load spectrum. In the analysis, a linear damage model, Miner's Rule, is used to demonstrate the prediction of the service lifetime for a typical wind turbine blade under assumed operating strain ranges and stress concentration factors. In contrast to typical European data, the asymmetry in this data base predicts failures under typical loads to be compressive.

INTRODUCTION

In recent papers, Mandell, et al. (1995) and Samborsky and Mandell (1996) brought together the extensive set of S-N fatigue data that was developed at Montana State University (MSU) under the auspices of the U.S. DOE's Wind Energy Program. The data base, herein called the MSU/DOE data base, now contains over 2200 data points with test results for typical U.S. wind turbine blade materials, i.e., E-glass fiber composites with polyester, vinyl ester and epoxy matrices and with a variety of fiber contents and architectures. Specimens were tested over a range of 10^3 to 5×10^8 cycles and at R values of 2, 10, -1, 0.5 and 0.1 (the R value is defined to be the algebraic ratio of the minimum stress S_{\min} to the maximum stress S_{\max} in one cycle). Supporting tests for ultimate tensile, ultimate compression, and modulus were also conducted for inclusion in the data base. The fatigue data are from constant-amplitude S-N tests that were

conducted using conventional coupon test procedures and a high-speed coupon test procedure. The latter testing procedure was developed at MSU especially for these tests to permit high-cycle fatigue testing in a timely manner, see Mandell, et al. (1994).

Mandell, et al. (1993) have demonstrated that the data from the various fiberglass composite materials in the data base may be characterized by a power law curve fit when they are normalized to the ultimate tensile or compressive strength of the composite. Starting with the normalized curve fits at various R values, a Goodman Diagram is constructed and then normalized to typical wind turbine blade properties. This normalization is required because the relatively small coupons in the data base perform significantly better than the relatively large composite structures used in typical blades.

To illustrate the use of these data, a Goodman Diagram is used by the LIFE2 fatigue analysis code [Sutherland and Schluter, 1989] for wind turbines to analyze the WISPER protocol load spectrum for a U.S. wind park environment, developed by Kelley (1995). Damage rates and service lifetime estimates are used to demonstrate that these data predict significantly reduced fatigue life when the composite is subjected to compression. Predictions are compared with analyses based on a Goodman Diagram developed by DeSmet and Bach (1994).

MATERIAL CHARACTERIZATION

The MSU/DOE Data Base

The initial S-N fatigue data base was reported by Mandell, Reed and Samborsky (1992). These fatigue data were obtained from constant-amplitude S-N tests using traditional coupon tests. The coupons were typically 25 to 50 mm (one to two inches) wide and 4 to 8 mm (an eighth to a quarter inch) thick. The internal hysteretic heating of these polymer based materials, combined

with their poor heat transfer characteristics limited the testing frequency to below 20 Hz. Typically, these tests were run at a frequency of 10 Hz.

To cover the entire range of interest for wind turbine applications, the S-N data must extend to a minimum of 10^8 cycles. Using traditional techniques, one test would require over one hundred days to complete. Thus, an appropriate fatigue data base for wind turbine applications would be very difficult and time consuming to build when tests are limited to 10 or 20 Hz cyclic rates. To overcome this difficulty, Creed (1993) and Mandell, et al. (1994) have developed a new testing technique that permits testing at frequencies up to 100 Hz, thus shortening the test period for 10^8 cycles to just eleven days. Adequate heat transfer is achieved in this technique by using relatively thin specimens, approximately 1.5 mm (0.06 inch) thick. This thickness limits the number of fiberglass layers to less than 10. Details of the test development and validation are discussed by Creed (1993) and Mandell, et al. (1995). The validation process included a detailed comparison of the S-N fatigue data produced using the relatively thin coupons to data produced using standard coupons. The comparison showed that the S-N data were within experimental scatter of one another.

The data base now contains over 2200 data points with test results for E-glass fiber composites with polyester, vinyl ester and epoxy matrices. Many of the specimens used in these tests were supplied by U.S. wind turbine blade manufacturers. Other specimens were constructed to systematically study the effect on fatigue properties of variations in composite structure, e.g., fiber content and reinforcement architecture. The data base contains test results that span a range of 10^3 to 5×10^8 cycles and R values of 2, 10, -1, 0.5 and 0.1. A typical data set for uniaxial fiber lay-ups and an R value of 0.1 is shown in Figure 1. Supporting tests for ultimate tensile, ultimate compression, and modulus were also conducted for inclusion in the data base.

Power Law Fit

The fiberglass composite data contained in the data base cover a wide range of properties. Mandell, et al. (1993) demonstrated that the constant amplitude, S-N fatigue data may be characterized by a power law curve fit of the form:

$$\frac{\epsilon}{\epsilon_o} = C N^{-(1/m)} \quad , \quad [1]$$

where ϵ is the maximum cyclic strain if the coupon fails in tension or the minimum cyclic strain if the coupon fails in compression, ϵ_o is the ultimate tensile strain ϵ_{uts} or ultimate compression strain ϵ_{ucs} (for tensile and compressive failure, respectively), N is the number of cycles to failure, and m and C are the curve fitting parameters. The mean fits for uniaxial fiber lay-ups are summarized in Table I. The fits for an R value of 0.1 are shown in Figure 1. In this table, the first set of parameters (labeled 1 to 10^8 cycles) are the best fit parameters when all of the S-N data and the ultimate strain are considered (the lead coefficient C has been set to one in these fits to reflect the correct ultimate strain of the material). The second set (labeled

10^3 to 10^8 cycles) are the parameters for fits to the S-N data with lifetimes that are greater than 10^3 cycles. The third set (labeled 10^5 to 10^8 cycles) are the parameters for fits to the data with lifetimes that are greater than 10^5 cycles. In the latter two sets, the value of C is not restricted to a value of one.

To obtain the “best” overall fit shown in Figure 2, the first set of parameters was used from 1 to 10^3 cycles, the second from 10^3 to 10^5 and the final from 10^5 to 10^{10} . At the intersections, an average value was used. Note that the data underlying these fits are limited to approximately 10^8 cycles. Thus, from 10^8 to 10^{10} cycles, the power law fits are extrapolations of the 10^5 to 10^8 data.

Goodman Diagram

The data cited in the previous section describe the normalized behavior of the composites. To use this characterization in a service lifetime calculation, ϵ_o is denormalized by the ultimate tensile (ϵ_{uts}) and compressive (ϵ_{ucs}) failure strain of the material under consideration. Typical values for industrial blade laminates are 2.7 percent and 1.5 percent, respectively [Mandell et al. 1995]. The normalized data presented in Figure 2 are scaled to these values to obtain the S-N diagram shown in Figure 3, and the Goodman Diagram shown in Figure 4. In Figure 4, the plot has been normalized to ϵ_{uts} using the ratio of 2.7 to 1.5 for the tensile-to-compressive ratio.

When comparing Figures 3 and 4, one notes that the Goodman Diagram is based on curve fits to the ultimate tensile and compressive strains and curve fits at five R values. Between these five constant R value lines, a Goodman Diagram has been constructed using straight lines. This construction technique is a reasonable approximation between R values of 2, 10 and -1 and the ultimate compressive strain, and between R values of 0.1 and 0.5 and the ultimate tensile strain, because the failure mechanisms for the former are all compressive and for the latter they are all tensile. However, somewhere between an R value of -1 and 0.1, the failure mechanism changes from compressive to tensile. The transition between the two is not defined in the data base. In the rendition of the Goodman Diagram shown in Figure 4, this region is also bridged with straight lines.

In Figure 5, the Goodman Diagram shown in Figure 4 has been redrawn with the tensile failure extension, indicated by the dashed line, into an R range of -1 to 0.1. As shown by this extension, a tensile failure mechanism in this range will produce significantly higher strains to failure. Thus, we have chosen a conservative estimate of a Goodman Diagram in this region.

In the FATigue of Composites for wind Turbines (FACT) data base [DeSmet and Bach, 1994], ϵ_{uts} and ϵ_{ucs} are 2.58 percent and 1.94 percent, respectively. These values produce an almost symmetric Goodman Diagram. A symmetric diagram implies that there are only small differences between tensile and compressive failures. For tensile failure (R values between 0 and 1), the two data sets are in general agreement. However, for compressive failures, there are significant differences in the strain to failure, with the MSU/DOE data base predicting lower strains to failure and shorter service lifetimes. The effects of

these differences on predicted service lifetimes are demonstrated below in the sample fatigue analysis.

The discrepancy in the compressive strain to failure between the two data bases may reflect the difference in the compression test methodology. In particular, the compressive tests conducted at MSU used gauge sections with no lateral constraints. Whereas, the FACT data base has a preponderance of data obtained from compression tests with lateral constraints.

WISPER PROTOCOL LOAD SPECTRA

The WISPER reference loading spectrum, herein called the European load spectrum, was developed by an international working group composed of thirteen different European research institutes and manufacturers [Ten Have, 1992]. The objective of the effort was to specify variable-amplitude (or spectral) test-loading histories that incorporate the major features seen in the root flapwise (out-of-plane) bending of horizontal-axis wind turbine (HAWT) blades. The European load spectrum is derived from eight load cases that are called “classes” or “modes.” The first two classes are the loads for discrete events, specifically turbine start-up (Class 1) and stopping (Class 2). The six remaining classes, 3 through 8, define the load histories for continuous operation of the turbines over their operating wind speed range. Class 3 contains representative data for mean wind speeds below 9 m/s. Classes 4 through 7 contain data for mean wind speeds of 9-11, 11-13, 13-15, and 15-17 m/s, respectively. Finally, Mode 8 describes the loads for mean wind speeds exceeding 17 m/s. Only classes 3 through 8 are used in the analyses presented here.

Kelley (1995) found that the WISPER development protocol could be successfully applied to the U.S. wind farm operating environment. As one might expect, the load spectrum from the wind farm analysis differed significantly from the European load spectrum, which is based on the loads from singly-sited turbines located in relatively smooth terrain. The U.S. wind farm load spectrum contained many more and larger loading cycles than the European load spectrum. And, Sutherland and Kelly (1995) showed that the wind farm load spectrum is significantly more damaging. Because this load spectrum is representative of a typical turbine in a U.S. wind farm, we will use the U.S. wind farm load spectrum to illustrate use of the data described above.

Both the European and the U.S. load spectra are normalized to an amplitude range of 1 to 64, with zero load equal to 25. To convert the normalized ranges to strains requires a detailed knowledge of design and loads on the turbine blade. Because we are not analyzing a particular turbine blade here, we assume that the maximum strain in the blade (which corresponds to amplitude range 64) is equivalent to a 0.4 percent strain level (this strain level is commonly used in the wind industry as the maximum allowable nominal strain for the blades).

As noted above, both spectra are bending moment spectra. Therefore, the blade is subjected to tensile strains on one side (up wind) and compressive strains on the other (down wind). The cyclic loads on both the tensile and compressive side are considered in this analysis.

FATIGUE LIFETIME PREDICTION

The LIFE2 code [Sutherland and Schluter, 1989] is a PC-based, menu-driven numerical analysis package that leads a user through the steps required to characterize the loading and material properties. Miner's rule or a linear crack propagation rule is then used to calculate the time to failure. Only Miner's rule is used here.

Input Parameters

The LIFE2 code requires four sets of input variables: 1) the wind speed distribution for the turbine site as an average annual distribution, 2) the material fatigue properties, 3) a joint distribution of mean strain and strain amplitude (or stress) for the various operational states of the turbine, and 4) a miscellaneous set of parameters that describe the operational parameters for the turbine (e.g., the cut-in and cut-out wind speed) and the stress concentration factor(s) for the turbine component. The reader is referred to Sutherland, Veers and Ashwill (1994) for a complete description of these input parameters.

For this analysis, we assume that the turbine is located at a Rayleigh site with an average wind speed of 6.3 m/s (14 mph). The material fatigue properties are the numerical equivalent of the data contained in the Goodman Diagram shown in Figure 4. For comparison, the Goodman Diagram developed from the FACT data base [DeSmet and Bach, 1994] is also used in the calculations. The third input data set is the U.S. wind farm load spectrum that is described above. Representative samples of the alternating component of the cyclic strain distribution, from the classes 5 and 7 wind speed bins, are shown in Figures 6a and 7a. Complete descriptions of these distributions are given by Kelley (1995). The fourth and final input set describes the operation of the turbine and the stress concentration factor. For these calculations, the turbine is assumed to operate between 5.4 m/s (12 mph) and 25 m/s (56 mph). The stress concentration factor is assumed to be 2.5.

Damage Calculations

The input parameters described above were used in the LIFE2 code to predict service lifetimes. The results of these analyses are summarized in Table II. They illustrate that the U.S. data base predicts the blade will fail in compression and at shorter lifetimes than predicted by the FACT data base. The former is due to the asymmetry in the Goodman Diagram of the MSU/DOE database, and the latter is due to the higher ultimate strains measured for the materials contained in the FACT data base.

To examine the asymmetry in greater detail, we will examine the damage rate produced by the U.S. wind farm strain spectrum in two typical wind speed bins, the classes 5 and 7 wind speed bins cited above and shown in Figures 6a and 7a. The damage associated with these strain distributions is shown in Figures 6b and 7b. In this case the damage \mathcal{D} at strain ϵ_i is defined by Miner's Rule to be

$$D(\mathbf{e}_i) = \frac{n[(\mathbf{e}_i)_a, (\mathbf{e}_i)_m]}{N[(\mathbf{e}_i)_a, (\mathbf{e}_i)_m]}, \quad [2]$$

where n is the number of cycles in the spectrum at alternating strain $(\mathbf{e}_i)_a$, mean strain $(\mathbf{e}_i)_m$ and N is the number of cycles at the same strain level. The total damage is simply the sum of the damage over all strain cycles in the spectrum. By Miner's Rule, failure occurs when the total damage accumulates to one.

As illustrated in Figures 6b and 7b and in Table II, compressive strains produce significantly more damage than equivalent tensile loads. This result is directly related to the strong asymmetry between compression and tension failures in the MSU/DOE data base that is characterized by the Goodman Diagram shown in Figure 4. Consider one component of strain load, namely the strain component shown in Figure 6 that is located near a nominal alternating strain amplitude of 0.3 percent. This component has a rate of accumulation of approximately 0.045 cycles per hour and nominal amplitude of 0.3 percent strain and a nominal mean of 0.1 percent strain. For tensile bending with a stress concentration factor of 2.5, this converts to 1.0 percent maximum strain and -0.5 percent minimum strain. For compressive bending, this converts to 0.5 percent maximum strain and -1.0 percent minimum strain. Thus, R equals -0.5 for tension and -2 for compression. As shown in the Goodman Diagram in Figure 5, the tensile failure strains to failure (see the R equal -0.5 dashed line in the Figure) are higher than the compressive failure strains (R equal -2 dashed line) for most alternating strains. This observation translates to a lower service lifetime in compression. Likewise, the approximately symmetric Goodman Diagram in the FACT data base produces a lower service lifetime in tension.

CONCLUDING COMMENTS

The MSU/DOE data base contains over 2200 data points with test results for fiberglass composites with polyester, vinyl ester and epoxy matrices and with a variety of fiber contents. These data may be characterized by a power law curve fit when normalized to their ultimate tensile and compression failure strains. The Goodman Diagram constructed from these data displays a significant asymmetry between the tensile and compressive failure zones. A similar diagram constructed from the FACT data base does not display a pronounced asymmetry.

The fatigue calculations presented here demonstrate the significance of the differences between the MSU/DOE and the FACT fatigue data bases. For the particular load spectrum used in this example, the data bases predict similar lifetimes in tension, but in compression, the data bases predict very different lifetimes. The FACT data base predicts the critical failure mode to be tensile and the MSU/DOE data base predicts the critical mode to be compressive. As discussed in detail above, these differences are a direct result of the asymmetric MSU/DOE Goodman Diagram and the approximately symmetric FACT Goodman Diagram. We hypothesize that the differences may be attributed to testing methods (lateral constraints). However, these differences may indicate that the materials contained in the

FACT data base are significantly different from those contained in the MSU/DOE data base. Until definitive tests are conducted, these differences will remain unresolved.

ACKNOWLEDGMENTS

This work is supported by the U.S. Department of Energy under contract DE-AC04-94AL85000.

REFERENCES

- Creed, R.F., Jr., 1993, *High Cycle Tensile Fatigue of Unidirectional Fiberglass Composite Tested at High Frequency*, M.S. Thesis, Dept. of Chemical Engineering, Montana State University, Bozeman.
- DeSmet, B.J. and P.W. Bach, 1994, *DATABASE FACT: Fatigue of Composites for Wind Turbines*, ECN-C--94-045, ECN, Petten, the Netherlands.
- Kelley, N.D., 1995, "A Comparison of Measured Wind Park Load Histories With The WISPER and WISPERX Load Spectra," *Wind Energy 1995*, SED-Vol. 16, ASME, p. 107.
- Mandell, J.F., Sutherland, H.J., Creed, R.J., Jr., Belinky, A.J., and Wei, G., 1995, "High Cycle Tensile and Compressive Fatigue of Glass Fiber-Dominated Composites," *ASTM, Sixth Symposium on Composites: Fatigue and Fracture*, in publication.
- Mandell, J.F., Creed, R.J., Jr., Pan, Q., Combs, D.W., and Shrinivas, M., 1994, "Fatigue of Fiberglass Generic Materials and Substructures," *Wind Energy 1994*, SED-Vol. 15, ASME, p. 207.
- Mandell, J.F., Reed, R.M., Samborsky, D.D., and Pan, Q., 1993, "Fatigue Performance of Wind Turbine Blade Composite Materials," *Wind Energy 1993*, SED-Vol. 14, ASME, p. 191.
- Mandell, J.F., Reed, R.M., and Samborsky, D.D., 1992, *Fatigue of Fiberglass Wind Turbine Materials*, SAND92-7005, Sandia National Laboratories, Albuquerque.
- Samborsky, D.D., and Mandell, J.F., 1996, "Fatigue Resistant Fiberglass Laminates for Wind Turbine Blades," *Wind Energy 1996*, ASME, in publication.
- Sutherland, H.J., and Kelley, N.D., 1995, "Fatigue Damage Estimate Comparisons for Northern European and U.S. Wind Farm Loading Environments," *Proceedings of WindPower '95*, AWEA, Washington, DC.
- Sutherland, H.J., and Schluter, L.L., 1989, "The LIFE2 Computer Code - Numerical Formulation and Input Parameters," *Proc. WindPower '89*, SERI/TP-257-3628, American Wind Energy Association, Washington, DC.
- Sutherland, H.J., Veers, P.S., and Ashwill, T.D., 1994, "Fatigue Life Prediction for Wind Turbines: A Case Study on Loading Spectra and Parameter Sensitivity," *Case Studies for Fatigue Education*, ASTM STP 1250, p. 174.
- Ten Have, A.A., 1992, *WISPER and WISPERX: Final Definition of Two Standardized Fatigue Loading Sequences for Wind Turbine Blades*, NLR-TP-91476U, National Aerospace Laboratory NLR, Amsterdam, the Netherlands.

Table I: Power law fit of the fatigue data for uniaxial fiber lay-ups.

R	Power Law Coefficients with Range of Applicability					
	1 to 10^8 Cycles		10^3 to 10^8 Cycles		10^5 to 10^8 Cycles	
	C	m	C	m	C	m
0.1	1	11.3	0.969	11.6	0.740	14.3
0.5	1	15.4	0.977	16.0	0.977	16.0
-1	1	14.9	1.124	13.2	1.124	13.2
10	1	18.0	0.862	22.5	0.802	24.9
2	1	31.2	0.859	47.8	0.802	61.7

Table II. Predicted service lifetime in years.

Bending Direction	U.S. Data Base	FACT Data Base
Tensile	44.9	67.5
Compressive	23.5	136.

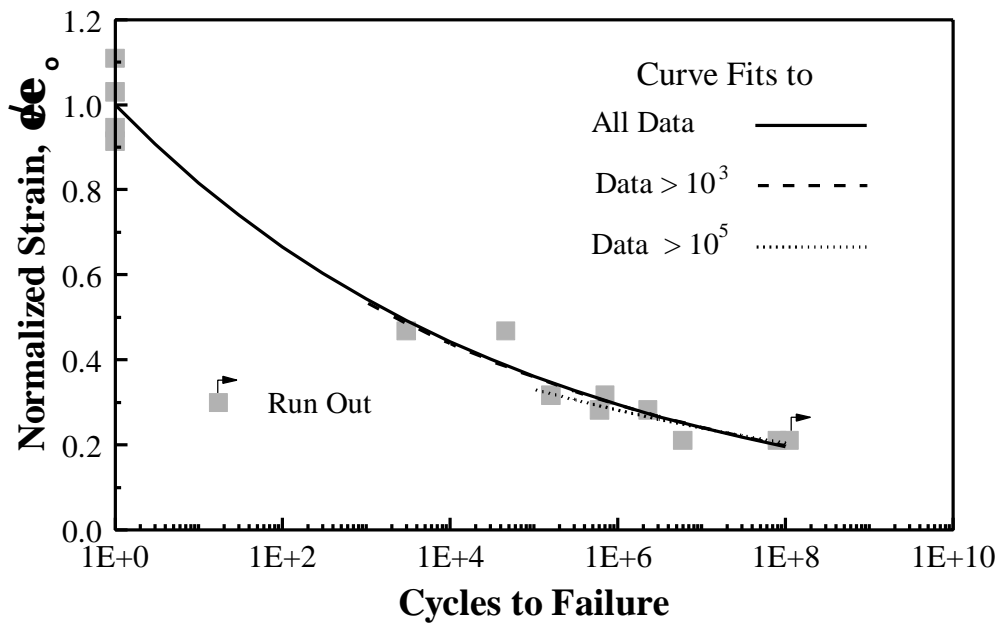


Figure 1. High cycle S-N data for R=0.1 with selected curve fits to the data.

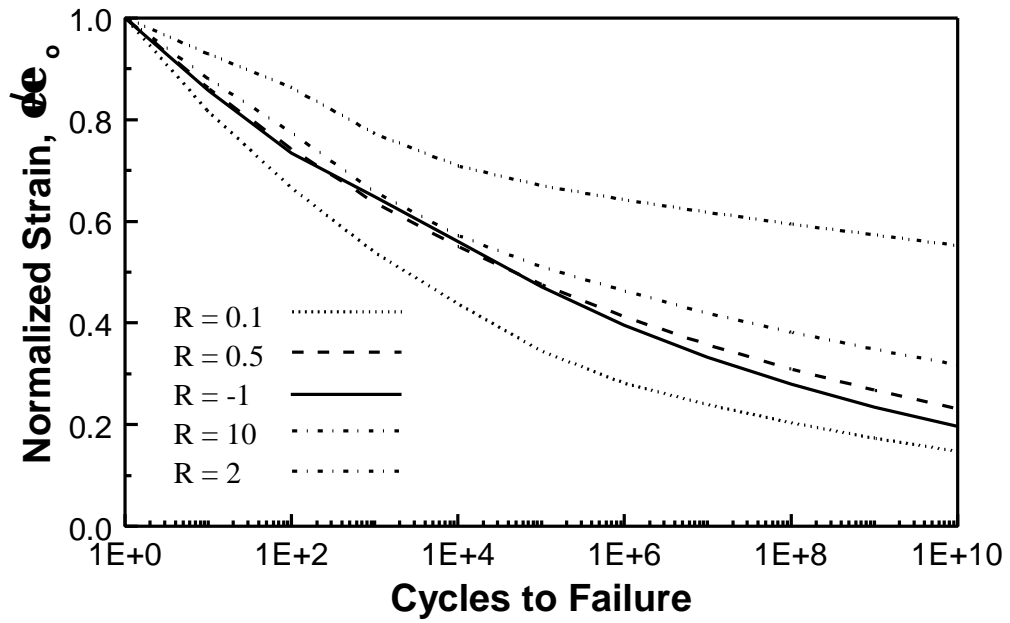


Figure 2a. Semilog plot.

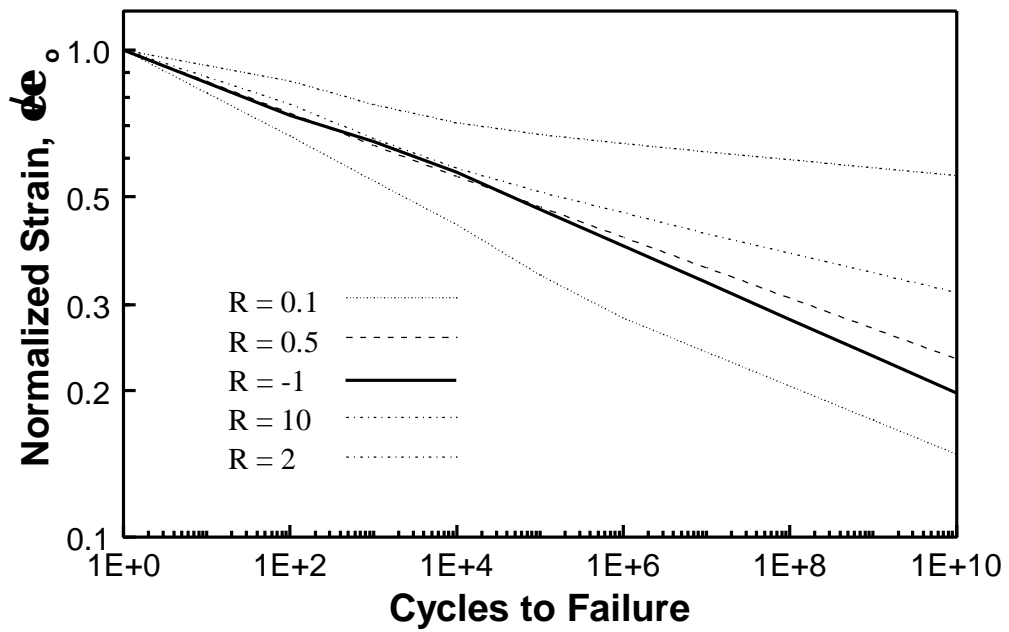


Figure 2b. Log-log plot.

Figure 2. S-N Diagram for fiberglass composites normalized to failure strain.

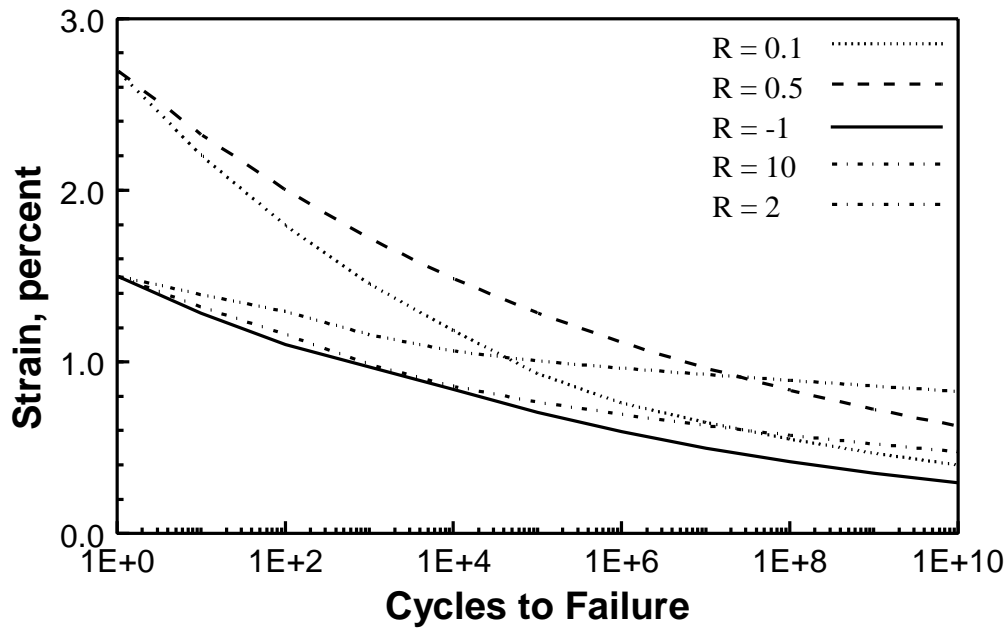


Figure 3. S-N Diagram for fiberglass composites based on the MSU/DOE data base.

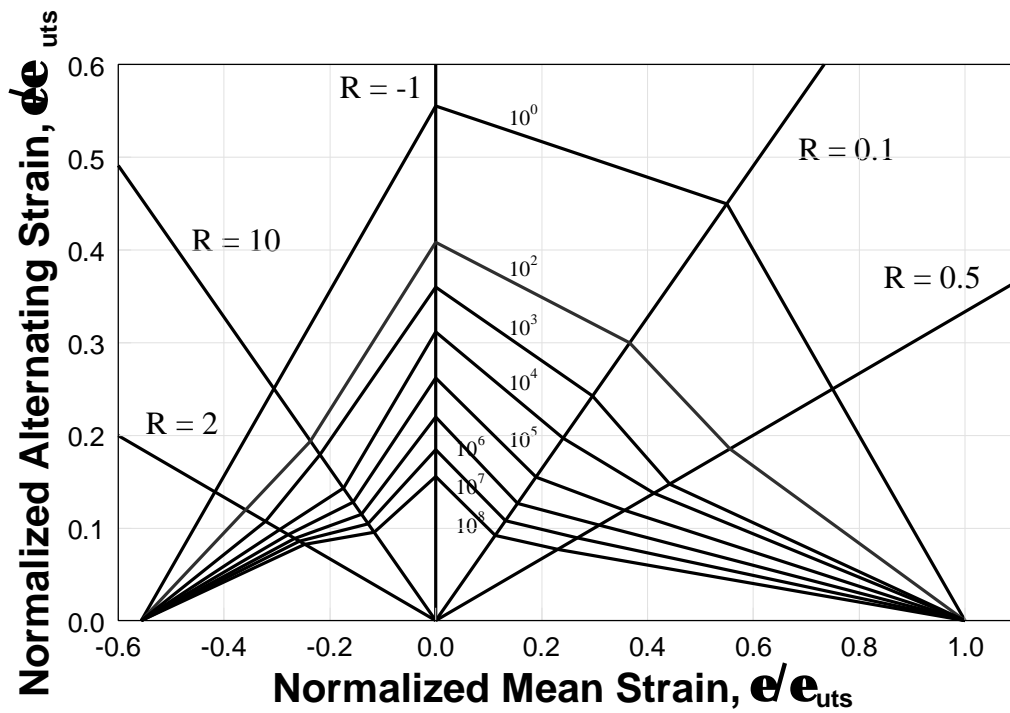


Figure 4. Normalized Goodman Diagram for fiberglass composites based on the MSU/DOE data base.

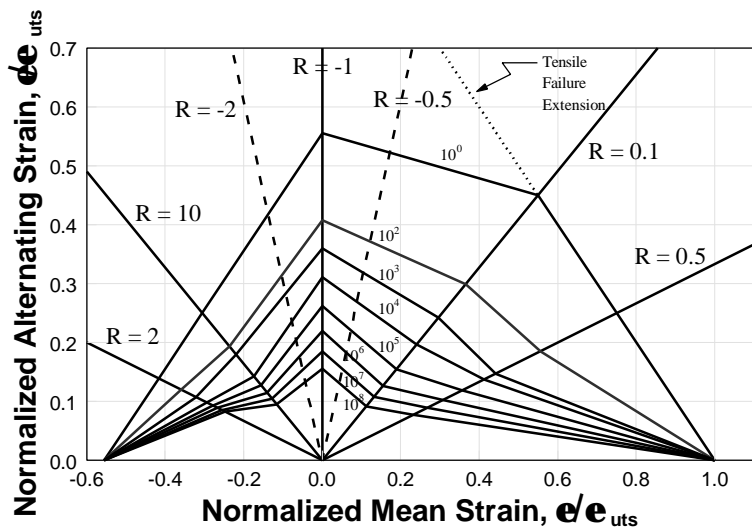
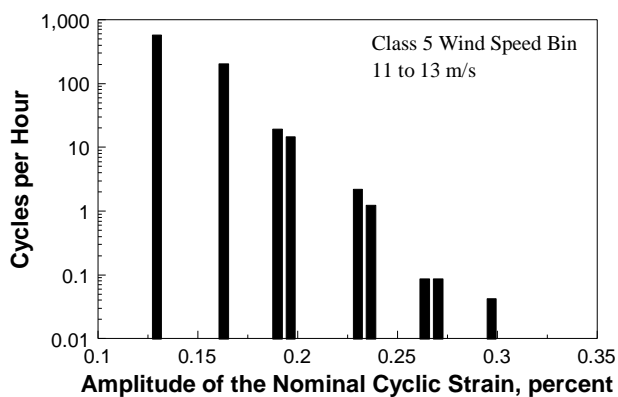
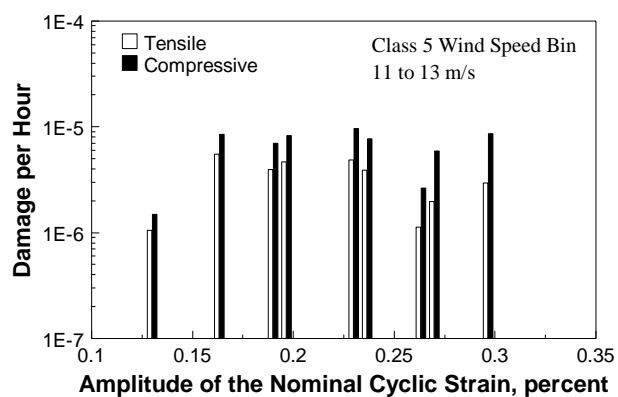


Figure 5. Goodman Diagram with tensile failure extension and constant R values based on the MSU/DOE data base.

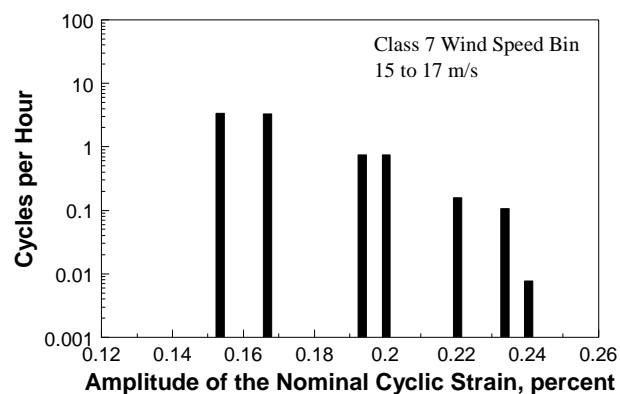


a. Strain spectra.

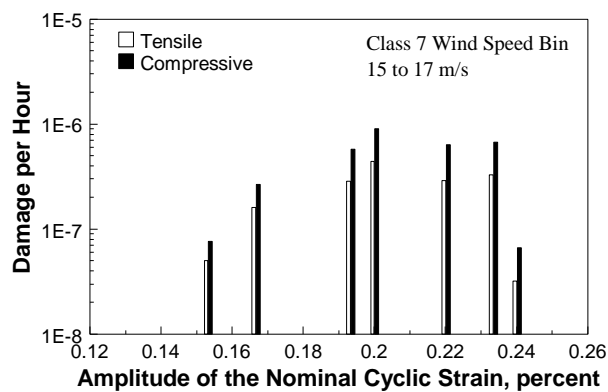


b. Damage spectra.

Figure 6. The U.S. wind farm load and damage spectra in the class 5 wind speed bin.



a. Strain spectra.



b. Damage spectra.

Figure 7. The U.S. wind farm load and damage spectra in the class 7 wind speed bin.